Anal Bioanal Chem
DOI 10.1007/s00216-010-3997-9

ORIGINAL PAPER

Ability of a salivary intrinsically unstructured protein to bind different tannin targets revealed by mass spectrometry

Francis Canon · Alexandre Giuliani · Franck Paté · Pascale Sarni-Manchado

Received: 23 April 2010 / Revised: 28 June 2010 / Accepted: 1 July 2010

Abstract Astringency is thought to result from the interaction between salivary proline-rich proteins (PRP) that belong to the intrinsically unstructured protein group (IUP), and tannins, which are phenolic compounds. IUPs have the ability to bind several and/or different targets. At the same time, tannins have different chemical features reported to contribute to the sensation of astringency. The ability of both electrospray ionization mass spectrometry and tandem mass spectrometry to investigate the noncovalent interaction occurring between a human salivary PRP, IB5, and a model tannin, epigallocatechin 3-*O*-gallate (EgCG), has been reported. Herein, we extend this method to study the effect of tannin chemical features on their interaction with IB5. We used five model tannins, epigallocatechin (EgC), epicatechin 3-*O*-gallate (ECG), epigallocatechin 3-*O*-gallate (EgCG), procyanidin dimer B2 and B2 3′-*O*-gallate, which cover the main tannin chemical features: presence of a gallate moiety (galloylation), the degree of polymerization, and the degree of B ring hydroxylation. We show the ability of IB5 to bind these tannins. We report differences in stoichiometries and in stability of the IB5•1 tannin complexes. These results demonstrate the main role of hydroxyl groups in these interactions and show the involvement of hydrogen bonds. Finally, these results are in line with sensory analysis, by Vidal et al. (J Sci Food Agric 83:564–573, 2003) pointing out that the chain length and the level of galloylation are the main factors affecting astringency perception.

Keywords Polyphenol · Noncovalent interaction · Proline-rich protein · Saliva · Astringency · Intrinsically unstructured protein

Abbreviations

CID	Collision-induced dissociation
EgC	Epigallocatechin
ECG	Epicatechin gallate
EgCG	Epigallocatechin gallate
B2 3′-OG	B2 3′-*O*-gallate
ESI	Electrospray ionization
IUP	Intrinsically unstructured protein
MS	Mass spectrometry
MS/MS	Tandem mass spectrometry
PRP	Proline-rich protein
*b*PRP	Basic proline-rich protein
*a*PRP	Acidic proline-rich protein
Q-TOF	Quadrupole/time-of-flight
T	Tannin
UGT	Ungalloylated tannin
GT	Galloylated tannin
M	Monomer
GM	Galloylated monomer
D	Dimer
GD	Galloylated dimer
DP	Degree of polymerization

F. Canon · F. Paté · P. Sarni-Manchado (✉)
INRA, UMR 1083 Sciences Pour l'Oenologie,
2, place Viala,
F-34060 Montpellier, France
e-mail: sarni@supagro.inra.fr

A. Giuliani
DISCO Beamline, Synchrotron Soleil,
l'Orme des Merisiers,
91192 Gif sur Yvette, France

A. Giuliani
CEPIA, INRA,
BP 71627, 44316 Nantes Cedex 3, France

Published online: 28 July 2010

Introduction

Over the last decade, the sequence-to-structure-to-function paradigm based on the view that proteins need to have a well-defined three-dimensional structure for their function, has been re-assessed. Numerous proteins do have a well-defined function that requires intrinsic disorder, and the term of intrinsically unstructured protein (IUP) has been proposed to describe this group [1]. IUPs appear to be rather common in living organisms, especially in higher eukaryotes: primary sequence analyses indicate that about 25% of full-length mammal proteins belong to this class [2]. The intrinsic lack of structure can confer functional advantages such as the ability to bind several and/or different ligands [1, 3, 4]. This ability often leads to mixtures of complexes with heterogeneous composition. While techniques are emerging for the characterization of flexible proteins [5, 6], the study of complexes of IUP is highly challenging and requires new approaches. Electrospray ionization (ESI) has demonstrated its efficiency to probe weak associations of molecules in solution such as receptor-ligand and protein-nucleic acid interactions [7, 8]. ESI-MS offers speed and sensitivity in monitoring components of mixtures and allows the determination of supramolecular edifices stoichiometry. Determination of relative binding affinities of noncovalent complexes is now well established [9–11]. Tandem mass spectrometry (MS/MS) provides access to noncovalent interaction strengths, and qualitative information on the complex structure [12, 13]. Herein, the ability of a model IUP, namely IB5, to form supramolecular edifices with different ligands is explored through MS and MS/MS approaches.

The IUP IB5 is a human salivary protein belonging to the class of proline-rich proteins (PRPs). For numerous mammals, PRPs are the most prevalent group of proteins in the saliva; they may constitute 70% of all proteins in human parotid saliva [14]. The salivary proteins play various roles (lubrication, digestion, taste, protection…) as saliva is the first fluid which interacts with food constituents. Salivary PRPs are classically divided in two groups, acidic PRPs (*a*PRPs) and basic PRPs (*b*PRPs) [15]. *a*PRPs act primarily in maintaining oral homeostasis, whereas the only known function of *b*PRPs is to bind and to scavenge tannins [16–18]. Moreover, in rats and mice, synthesis of salivary PRPs is stimulated by a tannin rich diet [19, 20]. PRPs affinity for tannins is estimated to be 5–80 and 1,000 times higher than that of bovine serum albumin and lysozyme, respectively [21–23]. PRP involvement in adaptation to tannin rich diet either as astringency mediator or/and as scavenger, is related to their ability to establish noncovalent interactions with tannins [15, 24].

Tannins are phenolic compounds ubiquitous in plant and plant-based foods and beverages. From a biological point of view, tannins act in plant defense mechanisms as molecules that protect against herbivores [25]. This role has been attributed to their ability to interact with proteins, to precipitate them and to inhibit gastrointestinal enzymes, thereby reducing the digestibility of plant proteins [26]. Proanthocyanidins are the main tannins in plant-based food (e.g., fruit, cocoa) and beverages (e.g. wine, tea, beer, cider…). These molecules have attracted considerable interest because of their quantitative importance and major contribution to organoleptic and biological properties. The chemical characteristics of proanthocyanidins are believed to affect their organoleptic properties, in particular their degree of polymerization, their level of B ring hydroxylation and their level of galloylation [27]. Numerous studies on the impact of these chemical characteristics over the protein•tannin interaction, were realized on poly L-proline [28] or peptides [29]. Since the affinity for tannins differs among proteins [22], PRPs [21] and with the length of PRP [30], it is essential to examine the effect of tannin chemical features on tannin interaction with a full basic salivary proline-rich protein (*b*PRP).

Our previous work on the interaction between IB5, a 70-a.a.-long human *b*PRP, and EgCG, a model tannin, revealed the presence in solution of IB5•EgCG supramolecular edifices with several stoichiometries [31]. The gas-phase stability of complex ions corresponding to two stoichiometries was investigated, and demonstrated the presence of several interaction sites on IB5. This approach affords the opportunity to estimate the ability of polyphenols to form different stoichiometry soluble complexes with a protein and to evaluate their stability. Since PRP–tannin interactions are thought to be involved in astringency [32], it is important to understand how the tannin chemical features have an effect on the stoichiometry, and on the strength of these interactions. To address these questions, we investigated the interactions between IB5, and five model tannins (T): three are monomers (M) epigallocatechin (EgC), epicatechin gallate (ECG), epigallocatechin gallate (EgCG), and two are dimers (D): B2 and B2 3′-*O*-gallate (B2 3′-OG; Fig. 1a). They cover the main chemical characteristics of tannins: number of units (DP), hydroxylation pattern of the B ring and presence of a galloylated moiety on position 3.

This paper describes the use of the ESI-MS CID approach developed previously, which has proven its efficiency to probe protein–tannin solution-state properties, to gain deeper understanding on the relation between tannin structure and astringency perception.

Materials and methods

Samples

Epigallocatechin (EgC), epicatechin gallate (ECG), epigallocatechin gallate (EgCG), and reserpine (Fig. 1a and b)

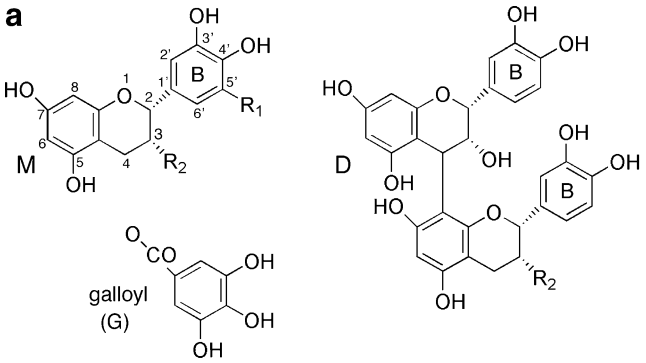

Tannins	skeleton	R_1	R_2
Epigallocatechin	M	OH	OH (UG)
Epicatechin gallate	M	H	galloyl (G)
Epigallocatechin gallate	M	OH	galloyl (G)
B2	D		OH (UG)
B2 3'OG	D		galloyl (G)

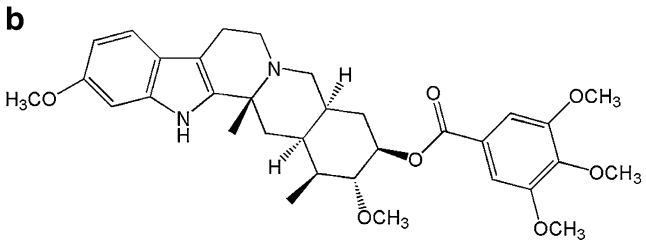

Fig. 1 Structures of **a** studied tannins (*T*) and **b** reserpine

were purchased from Sigma (Sigma Chemical Co., Poole, Dorset, U.K.). B2 and B2 3′-O-gallate were purified as previously described [33].

The human salivary proline-rich protein, IB5, was produced by use of the yeast *Pischia pastoris* as a host organism and purified as previously described [34].

Tannin and protein stock solutions were prepared in the following medium: water/ethanol, 88:12 (*v*/*v*) acidified to pH 3.2 with acetic acid. They were immediately frozen (−20 °C) to prevent protein proteolysis and tannin oxidation. Prior to use, they were diluted at room temperature to the desired concentrations.

Protein–tannin interactions

For IB5-tannin interactions, the protein concentration was kept constant at 5 μM in the water/ethanol medium described above. Tannins and protein solutions were mixed extemporaneously at room temperature (regulated at 24 °C) to obtain a protein/polyphenol molar ratio of 1:10.

The control solution, addressing the issue of nonspecific aggregates that could form during electrospray ionization, was prepared by mixing IB5 and reserpine at the same 1:10 final ratio as the IB5-T mixtures.

Electrospray ionization mass spectrometry and tandem mass spectrometry

Mass spectrometry and tandem mass spectrometry experiments were performed on a hybrid quadrupole time-of-flight (Q-TOF) Qstar Pulsar I mass spectrometer (Applied Biosystems, Forster City, CA), providing a resolving power of 10,000 at *m*/*z* 1080.8. The interface was fitted with the ion cooler guide to preserve the noncovalent complexes upon transfer into the gas phase. The ion cooler guide is mounted after the skimmer around Q0 and increases the local pressure to greater than 30 mTorr, which greatly improves preservation of weakly bound complexes [35]. The Q-TOF was operated with the Turbospray (electrospray ion source). The sample was infused in the mass spectrometer by means of a syringe infusion pump at 7 $\mu L.min^{-1}$ flow rate. The source voltage was set to 5,800 V in positive ion mode, the declustering potential at 47 V, the focusing potential at 209 V, the declustering potential 2 at 17 V, the ion source gas 1 set at 22, the ion source gas 2 at 0, the curtain gas at 10 and the capillary was not heated up. Nitrogen from a generator, containing less than 6 ppm oxygen was used both as nebulizing and desolvation gas. During MS/MS experiments, nitrogen was used as a collision gas in the collision cell (Linac) with CAD gas setting of 5. The collision-set energy voltage V_c was increased from 0 to 50 V. The kinetic energy of the precursor ion in the laboratory frame of reference is $E_{\mathrm{Lab}} = z \times e \times V_c$, where z is the number of charges on the ion and e is the charge of an electron [36].

Analysis of ESI-MS and MS/MS experiments and calculations

ESI-MS and collision MS/MS data were analyzed with Analyst QS [37] and MagTran [38] softwares.

A procedure adapted from Jørgensen et al. [39] and Wan et al. [40] was used to establish the dissociation curves. The 50% dissociation energy is defined as the energy giving a 50% loss of precursor complex ions. Based on the data of Akashi et al. [41], one of the multiprotonated molecules of the IB5•1tannin complex (M), $[M+6H]^{6+}$ was selected and submitted to CID.

Results and discussion

ESI-MS analysis of IB5•tannin complexes

The mass spectrum obtained by electrospraying the protein solution displayed a series of peaks corresponding to protonated isoforms of IB5 (a 6923.70, b 6642.63, and c 6360.39 Da) with charge states ranging from +5 to +10 as previously observed [31].

The concentrations chosen for protein and tannin reflect biological conditions. Concentrations of condensed tannins in red wine are approximately 1–2 $g.L^{-1}$, corresponding to a mean molar concentration of 0.5–1 mM. The concentration of proteins in saliva is approximately 1 $mg.mL^{-1}$ circa 83 μM. Polyphenols are present in large excess compared to proteins both in wine and in the mouth after sipping wine, making the protein/polyphenol ratio always in the benefit of polyphenols. On this basis, to investigate soluble protein–polyphenol complexes we use a protein/polyphenol ratio of 1:10 that gives rise neither to the formation of precipitate nor to cloudiness.

The interaction medium mimics the mouth condition during red wine consumption. As wine is more abundant than saliva, the buffering ability of wine tartaric acid leads to an acidic pH. The pH value of 3.2 used during this experiment is in the range of wine pH values, which are comprised between 2.8 and 3.8 [42, 43]. Moreover, the function of PRPs is to bind and scavenge tannins to protect digestive enzymes, for example in the stomach where pH is approximately 1.5 and PRP•tannin complexes are stable [44]. Thus, the pH used in this study reflects the biological pH of PRP–tannin interaction medium.

Premixed interaction medium with a 1:10 IB5/tannin molar ratio was submitted to ESI mass spectrometry. MS analysis reveals IB5•nT complex ion peaks for each mixture with several stoichiometries (*n* being the number of *T* molecules involved in the complexes, Fig. 2). Complexes involving galloylated tannins (IB5•nGT) show the highest stoichiometries and also the highest relative intensities. The presence of a galloylated moiety favors the interaction with IB5. Closer analysis of MS spectra shows that IB5•nUGT complexes (ungalloylated tannins) present similar stoichiometries, while stoichiometries of IB5•nGM complexes (galloylated monomers) are higher than those of IB5•nGD (galloylated dimers). This result may be related to the bulkier size of the dimers, which may restrict the number of sites that can be reached simultaneously on IB5. To address the issue of nonspecific aggregates, which could form during electrospray ionization, ESI mass spectra of mixtures of IB5 and reserpine have been recorded. Reserpine presents a chemical structure and a molecular mass close to those of our model tannins (Fig. 1). These spectra did not give rise to complex peaks. If the interaction was not driven by polyphenols, ESI-MS should have generated complexes between IB5 and reserpine. The absence of IB5•reserpine peak, and the presence of IB5•T peaks, demonstrated that the observed noncovalent complexes were not some ESI artifacts, sustaining the specificity of the protein–tannin interaction. The observation of IB5•T complexes demonstrates the ability of IB5 to bind different tannins. This result is in agreement with the characteristics of IUPs, which have often enough malleability to bind different partners [45, 46]. Observation of multiple and high stoichiometries is consistent with IB5 alleged function. The main function described for basic salivary PRPs, like IB5, is to be a scavenger that binds tannins [16–18, 47]. The extended structure of PRPs [48] allows them to bind more than one molecule of tannins to counteract their effects, especially when tannin concentration is rather high. These results confirm that PRP belong to the IUP functional class of scavenger [3, 49]. Scavenger IUPs work by molecular recognition and, can bind several partners at the same time [1, 3]. However, the stoichiometry differences observed among the complexes involving the different tannins reveal an impact of the tannin chemical features on the interaction. To pursue the investigation on this effect, the stability of IB5•1T complexes has been evaluated by MS/MS.

ESI-MS/MS analysis of IB5•1tannin complexes

The relative stability of IB5•1T complexes was investigated by monitoring $[IB5•1T]^{+6}$ ion dissociation by CID MS/MS experiments. Collision-induced dissociation is a multi-collisions process whereby precursor ions are activated upon collision with a non-reactive gas, nitrogen in the present case. Each collision increases the overall vibrational energy of the ion until there is enough internal energy accumulated within the species to overcome the bond dissociation energy, thus causing fragmentation [50]. In the present study, low-energy CID investigated the relative gas-phase stability of the noncovalent complexes $[IB5•1T]^{+6}$.

Ions were injected into the collision cell with increasing energies to dissociate them through collisions with nitrogen. Collision-induced total dissociation of all IB5•1T complexes gave rise to the ions corresponding to $[IB5]^{6+}$ and a neutral tannin.

$$[\mathrm{IB5} \bullet \mathrm{1T}]^{6+} \rightarrow [\mathrm{IB5}]^{6+} + \mathrm{1T}$$

Dissociation curves for each parent complex ion were derived and correlated the relative abundance of the parent ion to the collision energy (Fig. 3).

The maximum energy that ions can acquire in the collision cell is the center-of-mass collision energy (E_{CoM}) of each collision summed over all. Laboratory frame collision energies (E_{Lab}) are converted to center-of-mass energies by using the equation

$$E_{\mathrm{CoM}} = E_{\mathrm{Lab}} \frac{m_g}{m_g + m_i} \quad (1)$$

where m_{g} and m_{i} are the mass of the target gas and of the complex ion, respectively.

The number of collision (N_{col}) is determined by three parameters, the gas number density (n), the length of the

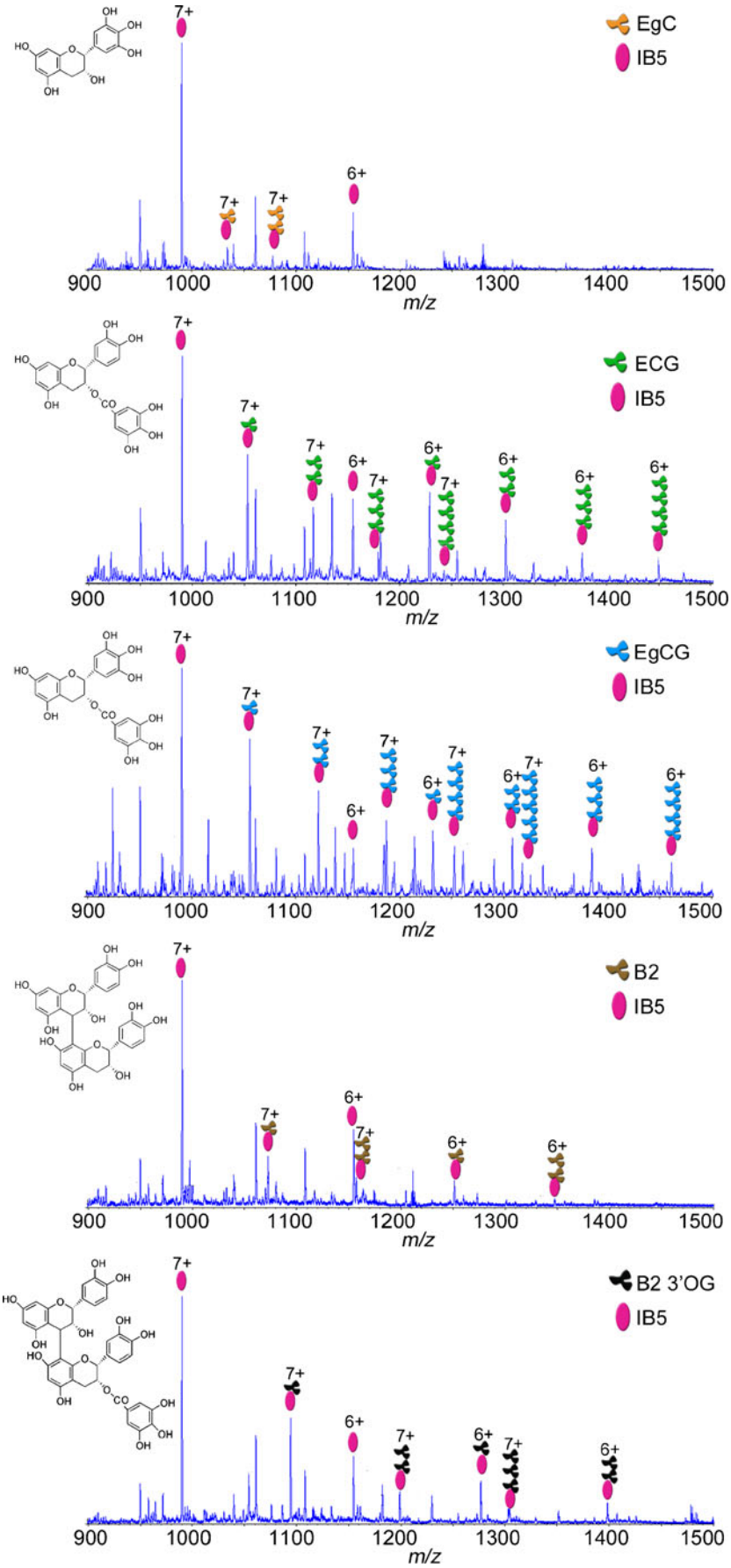

Fig. 2 Positive ion mass spectra of IB5:T (1:10) interaction mixtures. Peaks of IB5a and its complexes are labeled

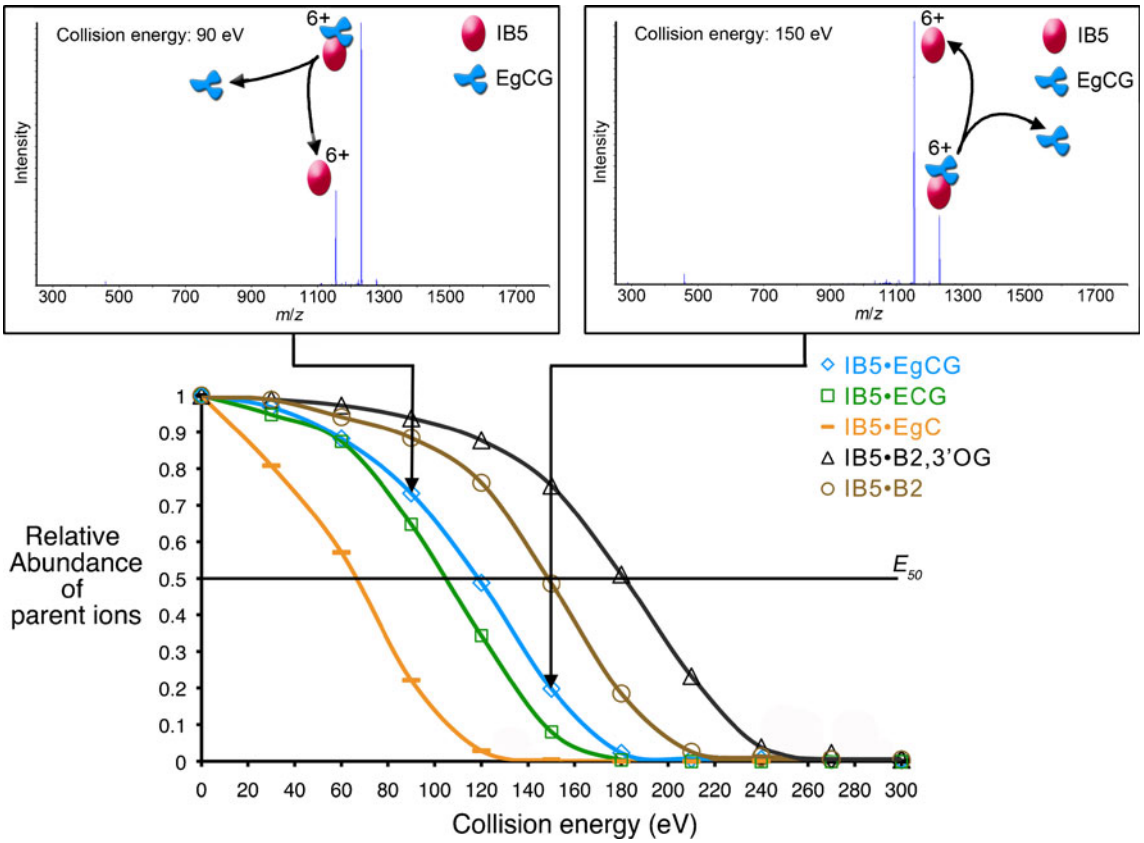

Fig. 3 Dissociation curves of $[IB5•1T]^{+6}$ and MS/MS spectra of $[IB5•1EgCG]^{+6}$ at collision energies of respectively 90 and 150 eV

collision cell (l) and the collision cross-section (σ) of the selected ion:

$$N_{col} = n \times \sigma \times l \quad (2)$$

Finally, the internal energy E_{Int} can be calculated from equation

$$E_{Int} = E_{CoM} \times N_{col} \quad (3)$$

Equation 2 shows that ions with similar cross-section experience the same number of collisions, on average. Thus from Eq. 3, direct comparison of E_{Int} can be realized via comparison of E_{CoM} for complexes with a similar collision cross-section. Given the slight modification of the molecular mass between $[IB5•1T]^{+6}$ complexes and their similar charge state [31, 51], we expect complex ions to present similar collision cross sections. Consequently, the center-of-mass energy of the complex (E_{CoM}) is likely to fit the scaling of the internal energy transferred to the complex upon dissociation.

The dissociation curves show similar sigmoid shape for each $[IB5•1T]^{+6}$, indicating that the interaction of IB5 with each tannin involves a similar mechanism independently of the tannin structure. During a first phase, dissociation curves depict an upper plateau where dissociation is minimal. Ions accumulate internal energy. Then, the curves bend downward into a log-linear dissociation region. Finally, the curves bend into a plateau toward the total complex dissociation. E_{50} in the laboratory frame is the

Table 1 E_{50} and E_{CoM} of the $[IB5•1T]^{+6}$ complexes

	IB5•EgC	IB5•ECG	IB5•EgCG	IB5•B2	IB5•B2, 3′-OG
E_{50} (eV)	67.5	105	120	150	165
E_{CoM} *(eV)*	0.26	0.40	0.45	0.55	0.65

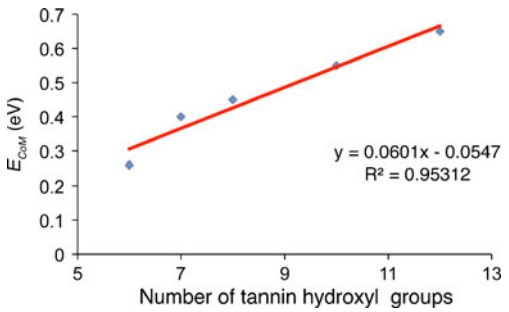

Fig. 4 Relation between the E_{CoM} of IB5•tannin complexes and the number of tannin hydroxyl groups

collision energy required to disrupt 50% of the parent complex ions. E_{50} are determined graphically from the dissociation curves (Fig. 3, Table 1). We used them to calculate the corresponding E_{CoM} (Table 1) reflecting complex stability [31, 51]. The higher the E_{CoM}, the stronger the interaction. Thus, classification of the complexes as a function of their stability can be drawn as:

$$[IB5 \bullet 1EgC]^{+6} < [IB5 \bullet 1ECG]^{+6} < [IB5 \bullet 1EgCG]^{+6} < [IB5 \bullet 1B2]^{+6} < [IB5 \bullet 1B2, 3'OG]^{+6}$$

It is worth noting that IB5•dimer complexes are more stable than those formed with monomers. Moreover, IB5•GT are more stable than IB5•UGT for a same degree of polymerization. The extra OH group on the B ring leads to a higher E_{CoM} (EgCG vs ECG). Through analysis of this set of tannins, we have shown the impact of chemical features on the stability of the complexes, and on the ability of IB5 to adapt to ligands, as previously observed for other IUPs [52]. Hence, we are able to classify these chemical characteristics as a function of their impact on the interaction strength with IB5:

B ring hydroxylation degree < galloylation < DP

Figure 4 shows that a linear relationship exists between the number of tannin hydroxyl groups and the E_{CoM} of IB5•tannin complexes. The more hydroxyl groups on tannins, the more stable the interaction with IB5. This indicates that interactions between IB5 and tannins mainly involve hydrogen bonds in the gas phase as stated earlier [31]. Electrostatic and hydrogen bonding interactions are enhanced in the gas phase whereas hydrophobic interactions are partly or completely lost [53, 54]. Therefore, the involvement of hydrophobic effect may not be excluded as it may occur in solution. Our results are in agreement with those of Simon [55], who has shown the importance of hydrogen bonding in the interaction between a proline-rich peptide (PRp: 14 a.a.) and tannins, with different techniques such as NMR, MS, CD, and molecular modeling.

Higher protein affinity has been reported for prodelphinidins (tannins with EgC units) compared to procyanidins (tannins mainly composed with EC and C units) [56]. In agreement with this finding, epigallocatechin gallate exhibited a stonger interaction than epicatechin gallate with immobilized salivary proteins [57]. The same trend was found when studying their complexation with the human salivary PRP IB5 by mass spectrometry but the reverse was found when calculating their binding constants with poly L-proline [58]. This difference can be explained by different affinities for tannins as observed between PRPs from various species [21] and by the random coil nature of *b*PRPs [48], which probably gives them enough malleability to be adaptable for different ligands in contrast with the polyproline helix conformation of poly L-proline.

Moreover, the astringency sensory analysis of different tannins has shown that DP and galloylation are major factors driving astringency perception [27]. This is parallel with our finding here, for which such factors are involved in the interaction strength with salivary proteins.

Conclusion

It is often asked why wine astringency sensation and intensity are dependent upon the wine itself and the wine taster. On one hand, wine molecules involved in astringency are tannins that gather a very large family of compounds with numerous and peculiar chemical structures. On the other hand, taster saliva holds a high level of proteins and particularly the so-called *b*PRPs whose only reported function is to bind tannins. Astringency is supposed to be related to their interactions and the stability of the arising complexes may have an impact on this perception. The stability of the complexes formed between tannins and *b*PRPs comes from the strength of the interaction forces. At this point, it makes compulsory to watch for them with regards to tannin chemical features. In this work, we used MS technologies benefiting from MS instrumentation developments to detect and characterize soluble noncovalent complexes involving a model *b*PRP, IB5, and tannins. The results show the effect of the tannin structure and highlight the involvement of hydrogen bounding on PRP–tannin interactions. The conformational rearrangement of PRP may favor the establishment of more hydrogen bonds. These results demonstrate the ability of PRP to universally bind tannins that have a variety of shapes and sizes and are in agreement with the tannin-scavenging function of IB5. Moreover, sensory analyses and MS studies have revealed that DP and galloylation are major factors driving tannin astringency perception [27] and PRP–tannin interaction respectively. This parallel is of particular interest because PRP–tannin interactions are thought to contribute to astringency mechanisms.

Acknowledgments The authors thank Dr. Véronique Cheynier for helpful scientific discussions, Thérèse Marlin for protein purification, Jean-Paul Mazauric for tannin purification and Emmanuelle Meudec for mass spectrometry assistance. Francis Canon was supported by a grant of French Ministry of Research. This work is supported by grant 07-BLAN-0279 from the French Agence Nationale de la Recherche (A.N.R.). We acknowledge synchrotron SOLEIL and thank all staff for assistance in using beamline DISCO. AG thanks ABSciex (Les Ullis, France) for the loan of the IonCooler Guide.

References

1. Dyson HJ, Wright PE (2005) Nat Rev Mol Cell Biol 6:197–208
2. Dunker AK, Silman I, Uversky VN, Sussman JL (2008) Curr Opin Struct Biol 18:756–764

3. Tompa P (2003) J Mol Struc (Theochem):361-371
4. Wright PE, Dyson HJ (1999) J Mol Biol 293:321–331
5. Bernstein SL, Dupuis NF, Lazo ND, Wyttenbach T, Condron MM, Bitan G, Teplow DB, Shea J-E, Ruotolo BT, Robinson CV, Bowers MT (2009) Nat Chem 1:326–331
6. Murray MM, Bernstein SL, Nyugen V, Condron MM, Teplow DB, Bowers MT (2009) J Am Chem Soc 131:6316–6317
7. Loo JA, Ogorzalek-Loo RR (1997) In: Cole RB (ed) Electrospray ionization mass spectrometry of peptides and proteins. Wiley, New York
8. Pramanik BN, Bartner PL, Mirza UA, Liu YH, Ganguly AK (1998) J Mass Spectrom 33:911–920
9. Jorgensen TJD, Roepstorff P, Heck AJR (1998) Anal Chem 70:4427–4432
10. Kapur A, Beck JL, Brown SE, Dixon NE, Sheil MM (2002) Protein Sci 11:147–157
11. Bligh SWA, Haley T, Lowe PN (2003) J Mol Recognit 16:139–148
12. Sobott F, McCammon MG, Robinson CV (2003) Int J Mass Spectrom Ion Processes 230:193–200
13. Jorgensen TJD, Hvelplund P, Andersen JU, Roepstorff P (2002) Int J Mass Spectrom Ion Processes 219:659–670
14. Mehansho H, Butler LG, Carlson DM (1987) Annu Rev Nutr 7:423–440
15. Bennick A (2002) Crit Rev Oral Biol Med 13:184–196
16. Carlson DM (1993) Crit Rev Oral Biol Med 4:495–502
17. Sarni-Manchado P, Canals-Bosch J, Mazerolles G, Cheynier V (2008) J Agric Food Chem 56:9563–9569
18. Sarni-Manchado P, Cheynier V, Moutounet M (1999) J Agric Food Chem 47:42–47
19. Mehansho H, Carlson DM (1983) J Biol Chem 258:6616–6620
20. Mehansho H, Clements S, Sheares BT, Smith S, Carlson DM (1985) J Biol Chem 260:4418–4423
21. Mole S, Butler LG, Iason G (1990) Biochem Syst Ecol 18:287–293
22. Asquith TN, Uhlig J, Mehansho H, Putnam L, Carlson DM, Butler L (1987) J Agric Food Chem 35:331–334
23. Austin PJ, Suchar LA, Robbins CT, Hagerman AE (1989) J Chem Ecol 15:1335–1347
24. McArthur C, Sanson GD, Beal AM (1995) J Chem Ecol 21:663–691
25. Dixon R, Xie D, Sharma S (2005) New Phytol 165:9–28
26. Zucker WV (1983) Am Nat 121:335–365
27. Vidal S, Francis L, Guyot S, Marnet N, Kwiatkowski M, Gawel R, Cheynier V, Waters EJ (2003) J Sci Food Agric 83:564–573
28. Poncet-Legrand C, Edelmann A, Putaux J-L, Cartalade D, Sarni-Manchado P, Vernhet A (2006) Food Hydrocoll 20:687–697
29. Sarni-Manchado P, Cheynier V (2002) J Mass Spectrom 37:609–616
30. Charlton AJ, Baxter NJ, Lilley TH, Haslam E, McDonald CJ, Williamson MP (1996) FEBS Lett 382:289–292
31. Canon F, Paté F, Meudec E, Marlin T, Cheynier V, Giuliani A, Sarni-Manchado P (2009) Anal and Bioanal Chem 395:2535–2545
32. Jobstl E, O'Connell J, Fairclough JPA, Williamson MP (2004) Biomacromolecules 5:942–949
33. Ricardo da Silva JM, Rigaud J, Cheynier V, Cheminat A, Moutounet M (1991) Phytochemistry 30:1259–1264
34. Pascal C, Bigey F, Ratomahenina R, Boze H, Moulin G, Sarni-Manchado P (2006) Protein Expr Purif 47:524–532
35. Yin S, Xie Y, Loo JA (2008) J Am Soc Mass Spectrom 19:1199–1208
36. Haller I, Mirza UA, Chait BT (1996) J Am Soc Mass Spectrom 7:677–681
37. Robinson CV (2001) J Am Soc Mass Spectrom 12:126–126
38. Zhang J, Kashket S (1998) Caries Res 32:233–238
39. Jørgensen TJD, Delforge D, Remacle J, Bojesen G, Roepstorff P (1999) Int J Mass Spectrom Ion Processes 188:63–85
40. Wan KX, Gross ML, Shibue T (2000) J Am Soc Mass Spectrom 11:450–457
41. Akashi S, Osawa R, Nishimura Y (2005) J Am Soc Mass Spectrom 16:116–125
42. Flanzy C (1998) Oenologie—Fondements scientifiques et technologiques. Lavoisier, Paris
43. Champagnol F (1986) Rev Fr Oenol 26:26–57
44. Shimada T (2006) J Chem Ecol 32:1149–1163
45. Fuxreiter M, Simon I, Friedrich P, Tompa P (2004) J Mol Biol 338:1015–1026
46. Oldfield C, Meng J, Yang J, Yang MQ, Uversky V, Dunker AK (2008) BMC Genomics 9:S1
47. Mehansho H, Hagerman A, Clements S, Butler LG, Rogler JC, Carlson DM (1983) Proc Natl Acad Sci USA 80:3948–3952
48. Boze H, Marlin T, Durand D, Pérez J, Vernhet A, Canon F, Sarni-Manchado P, Cheynier V, Cabane B (2010) Biophys J 99:656–665
49. Tompa P (2003) BioEssays 25:847–855
50. Khalsa-Moyers G, McDonald WH (2006) Brief Funct Genomic Proteomic 5:98–111
51. Chen Y-LC JM, Collings BA, Konermann L, Douglas DJ (1998) Rapid Commun Mass Spectrom 12:1003–1010
52. Wright PE, Dyson HJ (2009) Curr Opin Struct Biol 19:31–38
53. Robinson CV, Chung EW, Kragelund BB, Knudsen J, Aplin RT, Poulsen FM, Dobson CM (1996) J Am Chem Soc 118:8646–8653
54. Sobott FM, McCammon MG, Hernández H, Robinson CV (2005) Phil Trans R Soc A 363:379–391
55. Simon C, Barathieu K, Laguerre M, Schmitter JM, Fouquet E, Pianet I, Dufourc EJ (2003) Biochemistry 42:10385–10395
56. Hagerman AE (1989) In: Hemingway RW, Karchesy JJ (eds) Chemistry of tannin–protein complexation. Plenum, New York
57. Bacon JR, Rhodes MJC (1998) J Agric Food Chem 46:5083–5088
58. Poncet-Legrand C, Gautier C, Cheynier V, Imberty A (2007) J Agric Food Chem 55:9235–9240